Refereed Proceedings

The 12th International Conference on Fluidization - New Horizons in Fluidization Engineering

Engineering Conferences International *Year* 2007

Modeling of an Interconnected Fluidized Bed Reactor for Chemical Looping Combustion

Min Xu[*] Naoko Ellis[†]

Ho-Jung Ryu [‡] C. Jim Lim[**]

[*]The University of British Columbia, minx@chml.ubc.ca

[†]The University of British Columbia

[‡]Korea Institute of Energy Research

[**]The University of British Columbia, cjlim@chml.ubc.ca

Xu et al.: Fluidized Bed Reactor for Chemical Looping Combustion

MODELING OF AN INTERCONNECTED FLUIDIZED BED REACTOR FOR CHEMICAL LOOPING COMBUSTION

Min Xu, Naoko Ellis, Ho-Jung Ryu *, C. Jim Lim
Department of Chemical & Biological Engineering, University of British Columbia, 2360 East Mall, Vancouver, BC Canada V6T 1Z3
* Fluidization Research Center, Korea Institute of Energy Research, Daejeon 305-343, Korea

ABSTRACT

Chemical Looping Combustion (CLC) is comprised of two reactors, in which direct contact between air and fuel is avoided. A metal oxide, as oxygen carrier, transports oxygen from the air reactor to the fuel reactor while circulating between them. Based on the hydrodynamics coupled with reaction kinetics of oxygen carrier from the literature, a model for an interconnected fluidized bed reactor has been developed to optimize the design and operation of the reactor system. The model considers the chemical reaction of a single particle and a particle population balance for the calculation of bed particle conversion. The core-annulus and two-phase hydrodynamic models are assumed for the air and fuel reactors, respectively. Predictions of the oxygen emission, particle conversion and fuel conversion efficiency under different operating conditions are presented for a pilot scale CLC reactor system.

INTRODUCTION

As a promising way of integrating combustion, CO_2 separation and pollution control with high efficiency and low cost, Chemical Looping Combustion (CLC) has gained attention in recent years. As shown schematically in Fig. 1, the CLC is comprised of two reactors: a fuel reactor and an air reactor. The key to this technology is to develop an effective oxygen carrier and a reactor system. Different oxygen carriers (metal oxides) have been tested [Lyngfelt et al. (1)]. Some approaches have been presented for the reactor design and hydrodynamic studies [Lyngfelt et al. (1); Kronberger et al. (2); Kronberger et al. (3)]. The interconnected fluidized beds are believed to have the advantages over alternative designs [Lyngfelt et al. (1)]. However, there are few available reports [Adánez et al. (4)] on the mathematical model of the CLC reactor system to determine the critical variables for reactor design and operation. The particle population balance model has received some attention recently to describe the particles distribution in a circulating fluidized bed [Ramkrishna and Mahoney (5)]. Since the CLC reactor system is composed of a fast fluidized bed air reactor and a bubbling bed fuel reactor, a mathematical model can be developed by combining the fluidization properties and a particle population balance model for calculation of the bed particle conversion. The purpose of this paper is to develop a model for predicting the performance of the CLC reactor system, providing valuable data for reactor design and operation, and evaluating effect of the operation conditions and particle reactivity change.

The 12th International Conference on Fluidization - New Horizons in Fluidization Engineering, Art. 113 [2007]

MODEL DEVELOPMENT

Particle properties

Since one particle needs two properties to describe itself, i.e., solid conversion X (oxidation degree) and particle size R [Ishida et al. (6)], one solid mass distribution function can be introduced as $P(X,R)$, and the mass fraction of the particles with conversion between X and $X+dX$ and size between R and $R+dR$ can be expressed as $P(X,R)dXdR$. As the particles need the high mechanical strength to minimize the particle breakage, the particle size is assumed to be constant. Because the particle has porous structure and the gas penetrates into the particles through the particle grain to react with the active metal oxide (or metal) distributed evenly in space, we can further assume that the apparent volume of one particle remains constant and only the particle apparent density changes with the solid conversion. The particle apparent density can then be described by equation (1), according to definition of X [Lyngfelt et al. (1)]:

$$\rho_X = \rho_{100} - (1-X)(\rho_{100} - \rho_0) \quad (1)$$

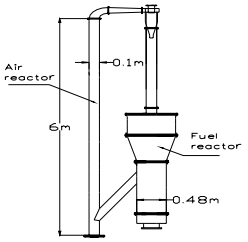

Fig. 1. Proposed CLC reactor system

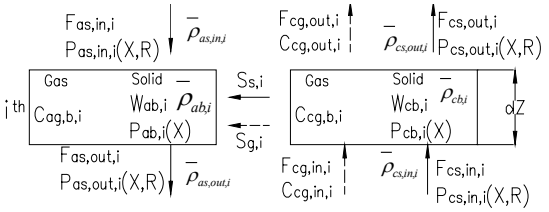

Fig. 2. Flow structure in air reactor

General particle mass balance equation

If a group of particles with mass of W in a fixed space volume can be described by the particle mass distribution function $P_b(X,R)$, and a solid stream F_0 with mass distribution function $P_0(X,R)$ is fed into the volume, and a solid stream F_1 with mass distribution function $P_1(X,R)$ is drained out from the volume, a mass balance on the particles with conversion between X and $X+dX$ and size between R and $R+dR$ in unit time is given as [Levenspiel et al. (7)]:

$$F_0 P_0(X,R) - F_1 P_1(X,R) - W\frac{d[P_b(X,R)\gamma(X,R,C)]}{dX} + \frac{WP_b(X,R)\gamma(X,R,C)}{a-(1-X)} = 0 \quad (2)$$

where $a = \frac{\rho_{100}}{\rho_{100}-\rho_0}$, $\gamma(X,R,C) = \frac{dX}{dt}$ is the reaction rate of particles at a given pressure and temperature. Since $\iint_{all\ X\ and\ R} P(X,R)dXdR = 1$, Integrating of equation (2) over all sizes and conversions gives:

$$F_0 - F_1 + \iint_{all\ X\ and\ R} \frac{WP_b(X,R)\gamma(X,R,C)}{a-(1-X)} = 0 \quad (3)$$

Particle population balance model in air reactor

The air reactor is characterized by a core-annulus structure, the hydrodynamics parameters can be referred to the literatures [Loffler et al. (8)]. As shown in Fig. 2, the air reactor is divided into a series of cells with height of dZ, for the ith cell, considering mass balance on particles with conversion between X and $X+dX$ and size between R and $R+dR$ in the core as the following:

$$F_{cg,i}P_{cg,i}(X,R) - F_{cg,i}P_{cg,i}(X,R) - W_{cb,i}\frac{d[P_{cb,i}(X,R)\gamma(X,R,C_{cg,b,i})]}{dX} + \frac{W_{cb,i}P_{cb,i}(X,R)\gamma(X,R,C_{cg,b,i})}{a-(1-X)} + S_{s,i}(X,R) = 0 \quad (4)$$

where: $S_{s,i}(X,R) = -[D_{ca}\frac{W_{cb,i}}{V_{cb,i}}P_{cb,i}(X,R) - D_{ac}\frac{W_{ab,i}}{V_{ab,i}}P_{ab,i}(X,R)]\pi r_{c,i}^2 dZ$

Integrating Equation (4) over all sizes and conversions gives:

$$F_{cs,in,i} - F_{cs,out,i} - D_{ca}\frac{W_{cb,i}}{V_{cb,i}} + D_{ac}\frac{W_{ab,i}}{V_{ab,i}} + \iint_{for\ all\ and\ R}\frac{W_{cb,i}P_{cb,i}(X,R)\gamma(X,R,C_{cg,b,i})}{a-(1-X)}dXdR = 0 \quad (5)$$

Similarly, the mass balance equation for particles with conversion between X and $X+dX$ and size of R and $R+dR$ in the annulus of the ith cell:

$$F_{as,in,i}P_{as,in,i}(X,R) - F_{as,out,i}P_{as,out,i}(X,R) - W_{ab,i}\frac{d[P_{ab,i}(X,R)\gamma(X,R,C_{agb,i})]}{dX} + \frac{W_{ab,i}P_{ab,i}(X,R)\gamma(X,R,C_{agb,i})}{a-(1-X)} - S_{s,i}(X,R) = 0 \quad (6)$$

Integrating Equation (6) over all sizes and conversions gives:

$$F_{as,in,i} - F_{as,out,i} + D_{ca}\frac{W_{cb,i}}{V_{cb,i}} - D_{ac}\frac{W_{ab,i}}{V_{ab,i}} + \iint_{for\ all\ and\ R}\frac{W_{ab,i}P_{ab,i}(X,R)\gamma(X,R,C_{ag,b,i})}{a-(1-X)}dXdR = 0 \quad (7)$$

For the mass balance of oxygen in core region of the ith cell, we have equation:

$$F_{cg,out,i} - F_{cg,in,i} = -(\iint_{all\ X\ and\ R}\frac{W_{cb,i}P_{cb,i}(X,R)r(X,R,C_{cg,b,i})dXdR}{a-(1-X)} + S_{g,i}) \quad (8)$$

where: $S_{g,i} = K_{ca}(C_{cg,b,i} - C_{ag,b,i})2\pi r_{c,i}dZ$

There is no axial flow of gases in the annulus, the mass balance of oxygen in annulus region of the ith cell gives: $S_{g,i} = \iint_{all\ X\ and\ R}\frac{W_{ab,i}P_{ab,i}(X,R)\gamma(X,R,C_{ag,b,i})dXdR}{a-(1-X)}$ (9)

Assuming that the gases and solid are well mixed, we have:

$P_{cb,i}(X,R) = P_{cs,out,i}(X,R)$, $P_{ab,i}(X,R) = P_{as,out,i}(X,R)$, $\overline{\rho}_{cb,i} = \overline{\rho}_{cs,out,i}$, $\overline{\rho}_{ab,i} = \overline{\rho}_{as,out,i}$, $C_{cg,out,i} = C_{cg,b,i}$

The boundary conditions are:

At $Z = 0$: for solids, $F_{cs,in,1} = F_{s0}$, $P_{cs,in,1}(X,R) = P(X,R)_0$ $\overline{\rho}_{cs,in,1} = \overline{\rho}_{s0}$, $F_{as,out,1} = 0$

for oxygen, $F_{cg,in,1} = F_{g0}$, $C_{cg,in,1} = C_{O_2 0}$

At $Z = H$: for solids $F_{as,in,L} = 0$

Particle population balance model in fuel reactor

The fuel reactor model development is based on the assumption that it is operating as a bubbling fluidized bed with two phases. The solids in the emulsion phase are assumed to be completely mixed. The determination of hydrodynamic parameters in the fuel reactor can be referred to the literature [Donald (9)]. The flow structure can be simplified as shown in Fig. 3. For the fuel mass balance over a differential height of dZ, in the bubble phase, we have:

$$\frac{d(U_{abs}C_{fuel,B})}{dZ} = K_{be}a_b(C_{fuel,e} - C_{fuel,B}) \quad (10)$$

and in the emulsion phase,

$$(1-\delta)U_{mf}\varepsilon_{mf}\frac{dC_{fuel,e}}{dZ} = \delta a_b K_{be}(C_{fuel,B} - C_{fuel,e}) - \frac{1}{\alpha}(1-\varepsilon_{mf})(1-\delta)\overline{\rho}_{Bb}\iint_{all\ X\ and\ R}\frac{P_{Bb}(X,R)\gamma(X,R,C_{fuel,e})dXdR}{a-(1-X)} \quad (11)$$

The Boundary condition at $Z = 0$ $\quad C_{fuel,B,in} = C_{fuel,e,in} = C_0$

As shown in Fig. 3, considering the population of a group of particles with conversion between X and $X+dX$ and size between R and $R+dR$, the solid mass balance can be written as: $F_0P_0(X,R) - F_1P_1(X,R) - F_2P_2(X,R) + F_rP_r(X,R) - W_{Bb}\frac{d[P_{Bb}(X,R)\gamma(X,R,C_{fuel,e})]}{dX} + \frac{W_{Bb}P_b(X,R)\gamma(X,R,C_{fuel,e})}{a-(1-X)} = 0$ (12)

Integrating Equation (12) over all sizes and conversions gives

$$F_1 + F_2 - F_r - F_0 = \iint_{all\ X\ and\ R}\frac{W_{Bb}P_{Bb}(X,R)\gamma(X,R,C_{fuel,e})dXdR}{a-(1-X)} \quad (13)$$

The entrainment solid flow F_2, the recycle solid flow F_r can be expressed by the elutriation constant and cyclone efficiency. Considering the well mixed flow in the bed, we have:

$P_{Bb}(X,R) = P_f(X,R)$ and $\bar{\rho}_{Bb} = \bar{\rho}_f$

The mass of particles in the bed is: $W_{Bb} = \bar{\rho}_{Bb} \int_0^{H_f} A_f(1-\delta)(1-\varepsilon_{mf})dZ$ (14)

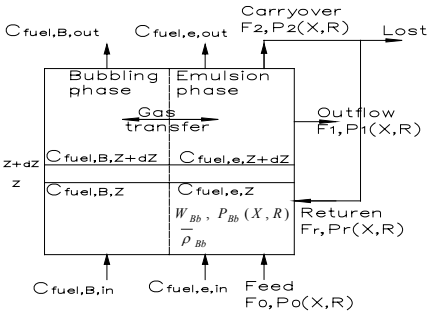

Fig. 3. Flow structure and solid flows in fuel reactor

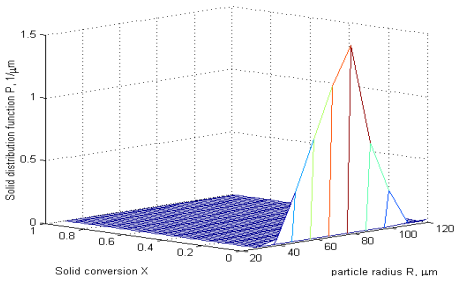

Fig. 4. Solid mass distribution function of inputting particles

Reaction rate of single particle

From the available published equations on reaction rate of single particles, the following reaction rates equations of NiO/YSZ particle oxidation and reduction proposed by Ishida et al. (8) were adapted. These equations were developed based on the packed bed experimental data using particle sizes between 1 to 3.2 mm.

$$\gamma(X,R,C_{O_2}) = \frac{dX}{dt} = \frac{6C_{O_2} \times 1000 / \rho_{Ni} \times 32}{\frac{1}{RK_{g,o}} + \frac{(1-X)^{-\frac{1}{3}} - 1}{D_{e,o}} + \frac{1}{RK_{s,o}}} \quad (15)$$

$$\gamma(X,R,C_{fuel}) = \frac{dX}{dt} = \frac{3b \times 1000 \times C_{fuel} / \rho_{Ni}}{\frac{R}{K_{g,r}} + \frac{R^2(X^{-\frac{1}{3}} - 1)}{D_{e,r}} + \frac{RX^{-\frac{2}{3}}}{K_{s,r}}} \quad (16)$$

where coefficients, D_e , K_g ,and K_s are given by Ishida et al. (6).

RESULTS AND DISCUSSION

According to the above rate equations, the oxidation rate is higher with lower solid conversion and reduction rate is higher with higher solid conversion. This is because both cases represent the reactions in the outer layer of particles. Therefore for the following simulation, the solid conversion of input particles of air and fuel reactors, whose solid distribution functions are shown in Fig. 4 and Fig.10, are set as 0~2% and 98%~100%, respectively. We choose a pilot scale CLC reactor system shown in Fig. 1, which consists of an air reactor with diameter of 0.1 m and height of 6 m and a fuel reactor with diameter of 0.48 m for simulation. Because of the kinetic rate data [Ishida et al. (6)] used for this simulation, we assume that the operating temperatures are 1273K and 873K for the air reactor and fuel reactor, respectively, oxygen and H_2 are used as reactants. The purpose of this section is to test whether the model gives expected responses to certain model parameters such as pressure, superficial gas velocity, and solids circulation rate and solids inventory.

Simulations for air reactor

This section examines the oxygen profile along the reactor height as a function of operating conditions for reactor design purposes. Fig.5 indicates that higher superficial gas velocity requires larger air reactor height to absorb more input oxygen. This is to compensate for the decrease in the mean residence time of oxygen with increasing superficial gas velocity. Compared with increasing superficial gas velocity, operating

reactor under high pressure is a better solution to provide more oxygen for the CLC reactor system. As shown in Fig. 6, when the pressure is increased from 0.1 MPa to 1.0 MPa (which means 900% increase in oxygen mass flow rate), the reactor height of 3.5 m is enough for complete conversion of oxygen. Fig. 7 shows the output oxygen concentration is strongly depended on the solid circulation rate, especially when the reactor operates under high pressure.

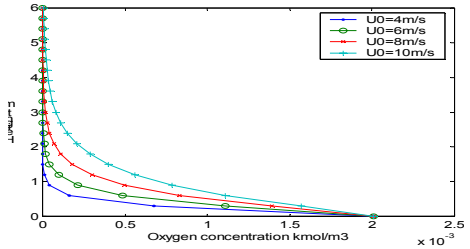

Fig. 5. Oxygen concentration distribution the core for different superficial gas velocity (Pressure=0.1MPa, G_s=100kg/m^2.s, T=1273K)

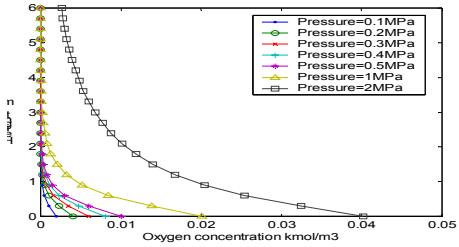

Fig. 6.Oxygen concentration distribution in the core for different pressure (U_0 =6m/s, G_s =100kg/m^2.s, T=1273K)

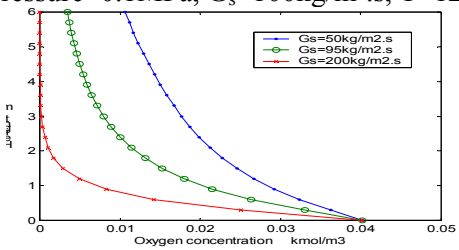

Fig. 7. Oxygen concentration distribution in the core for different solid circulation rate (U_0 =6m/s, pressure=2.0MPa, T =1273K)

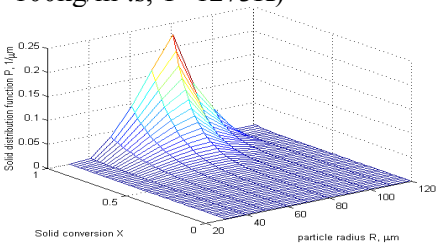

Fig. 8. Solid mass distribution functions of input particles A

Simulation for fuel reactor

Effect of mass solid distribution function of input particles

Input particles that have the different mass solid distribution function may result in different fuel conversion efficiency even if they have the same average solid conversion and average particle size. Figs. 8 and 9 show two input streams of solids, A and B, which have the same average solid conversion (87.5%) and the same average particle size (149 μm) with different solid mass distribution functions. Most of the particles in Solid stream B are in the higher solid conversion range which has a higher reduction rate [Ishida et al. (6)], as a result, solid stream B can achieve higher fuel conversion efficiency. Under the conditions of U_0=0.15m/s, pressure=0.1MPa,T=873K,G_s=100kg/m^2.s and W=102kg, fuel conversion efficiencies for solid streams A and B are 79.0% and 95.7%, respectively.

Effect of superficial gas velocity, pressure, solid circulation rate and bed loadings

In this section, we have applied two different reduction reaction rates: the higher reaction rate is calculated from Equation (16), while the low reaction rate is taken as 1% of the higher reaction rate. Fig. 11 allows us to examine the maximum superficial gas velocity to achieve 100% fuel conversion for a given solids circulation rate and it shows that with increasing superficial gas velocity, the fuel conversion efficiency deceases. This is because higher superficial gas velocity means higher fuel mass flow rate and less reaction time of fuel. For the lower reaction rate, the extent of decrease of fuel conversion efficiency is more

The 12th International Conference on Fluidization - New Horizons in Fluidization Engineering, Art. 113 [2007]

significant. The results in Fig. 12 indicate that fuel can be completely consumed for high reaction rate when pressure is increased from 0.1 MPa to 1.0 MPa. However when the pressure is further increased to 2.0 MPa, the fuel conversion efficiency is decreased to 68.3%. Under these conditions, the output particles have been completely converted, and there is no oxygen remaining in the reacted particles. However, for the case of the low reaction rate, the fuel conversion efficiency is mainly controlled by the reaction rate at high pressure as the calculation indicates reductions in the solid conversion of output particles to 33.7% and 9.6% for pressures of 0.1 MPa and 2.0 MPa, respectively.

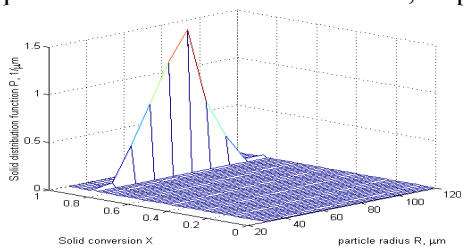

Fig. 9. Solid mass distribution functions of input particles B

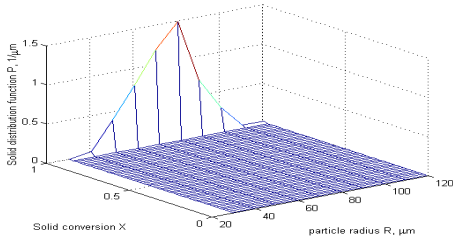

Fig. 10 .Solid mass distribution function of input particles

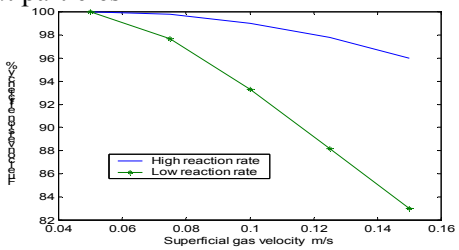

Fig.11.Fuel conversion efficiency for different superficial gas velocity (Pressure=0.1 MPa, T=873K, Gs=100kg/m^2.s, W=119 kg)

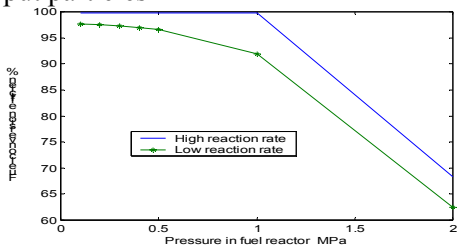

Fig.12.Fuel conversion efficiency for different pressure in fuel reactor (U_0 = 0.075 m/s,T=873K,Gs=100 kg/m^2.s,W=119kg)

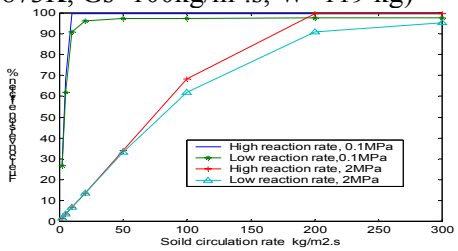

Fig. 13. Fuel conversion efficiency for different solid circulation rates (U_0 = 0.075 m/s, T = 873 K, W = 110 kg, Pressure = 0.1 MPa and 20 MPa)

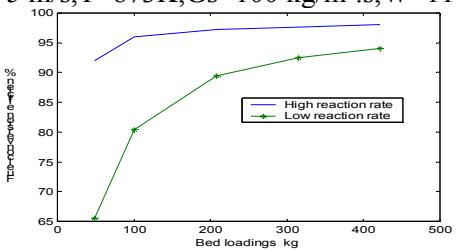

Fig. 14. Fuel conversion efficiency for different bed loadings in fuel reactor (U_0 = 0.15 m/s, Pressure = 0.1 MPa, T = 873 K, Gs = 100 kg/m^2.s)

As shown in Fig. 13, increasing solid circulation rate can improve the fuel conversion efficiency significantly for both the high and low reaction rates. For a given bed loading, a small solid circulation rate means a larger mean particle residence time which leads to a higher conversion of particles. However, if the solid circulation rate is too small, there is not enough oxygen in the particles to achieve high fuel conversion efficiency. Increasing solids circulation will reduce the mean particle residence time in the fuel reactor and therefore, solids inventory. The higher total solids transferred between fuel reactor and air reactor will provide enough oxygen to achieve higher fuel conversion efficiency, even for the low reaction rate. From Fig. 14, fuel conversion efficiency is a strong function of bed loading especially for the low reaction rate. For the high reaction rate, the effect of bed loadings is not significant owing to the particles attaining enough conversion within a short residence time.

INTERCONNECTION OF AIR REACTOR AND FUEL REACTOR

Under the typical testing operation conditions in Table 1, for a steady-state interconnected fluidized bed reactor shown in Fig. 1, we can obtain the results shown in Table 1. In this case, the heat capacity of the CLC reactor system is 45 KW. The solid conversion difference is 7.1%. The temperatures in the air reactor and fuel reactor as 1273K and 873K, respectively, were chosen based on the kinetic data available [Ishida et al. (6)].

For this particular case study, the fuel reactor can consume more fuel with higher solid conversion difference of particles at any specific solid circulation rate, and the corresponding higher solid conversion difference cannot be compensated in the air reactor since the air superficial velocity cannot be increased unlimitedly under atmospheric pressure. Therefore, the power capacity of the CLC reactor system depends on the maximum amount of oxygen which can be absorbed by particles in the air reactor.

Table 1 Typical testing operation conditions and results

Conditions			
Solid circulation rate	100 kg/m^2.s	Bed height of fuel reactor	0.5m
U_0 for air reactor	6 m/s	Pressure	0.1 MPa
U_0 for fuel reactor	0.075 m/s	Temp. in air reactor	1273 K
Bed loading in fuel reactor	113.6 kg	Temp. in fuel reactor	873 K
Result for air reactor		**Result for fuel reactor**	
$\overline{X}$ of input particles	91.9%	$\overline{X}$ of input particles	99%
$\overline{X}$ of output particles	99%	$\overline{X}$ of output particles	91.9%
Oxygen conversion efficiency	100%	Fuel conversion efficiency	99.8%

CONCLUSION AND SUMMARY

- Particles in the fuel reactor with different solid mass distribution functions will result in different fuel conversion efficiency, even though they may have the same average solid conversion and average particle size.
- If the reaction rates are high enough, the fuel conversion efficiency and the oxygen available for combustion have a strong dependency on the solid circulation rate. But if the reaction rates are low, the performance of reactor system mainly controlled by the reaction rates.
- If the required power capacity and working pressure are determined, the model can predict the minimum solid circulation rate, bed loadings, bed dimensions and appropriate superficial gas velocity under the conditions of complete fuel conversions.

ACKNOWLEDGEMENT

The financial support from the Nature Science and Engineering Research Council of Canada is gratefully acknowledged.

NOTATIOIN

a_b :Bubble surface area per unit volume. b :Stoichiometric coefficient of solid reactant (-)

C :Gas concentration (kg/m^3 for oxygen, kmol/m^3 for fuel)

D_{ca}:Solid transfer coefficient from core to annulus (m/s)

D_{ac} :Solid transfer coefficient from annulus to core (m/s)

F : Mass flow rate (kg/s for solid and oxygen, kmol/s for fuel)

G_s :Solid circulation rate (kg/m^2.s) H : Height of bed (m)

K_{be} : Gas transfer coefficient between bubble and emulsion (m/s)

P : Solid mass distribution function ($_{\mu m^{-1}}$) r :Radius of core (m) R : Particle radius (m)

S : Mass flow rate of solid or oxygen transferred from core to annulus (kg/s for solid, kmol/s for oxygen)

T : Temperature (K) U : Velocity of gas or solid (m/s) U_0 : Superficial gas velocity (m/s)

V : Volume (m^3) W : Mass of the solid in a bed or in a space volume (kg)

X : Solid conversion of particle (Oxidation degree) (-), $\overline{X}$: Average solid conversion (-)

Z : Location of bed along the height (m)

ρ : Particle density (kg/m^3) $\overline{\rho}$: Average particle density (kg/m^3)

ρ_{100} , ρ_0 , ρ_X : Apparent density of particle with X of 100%, 0% and X respectively(kg/m^3)

α : Mass of oxygen for complete conversion of 1 kmol fuel (kg)

γ : Reaction rate, i.e. $\frac{dX}{dt}$ (s^{-1}) δ : Volumetric fraction of bubbles (-) ε : Voidage (-)

Subscripts:

0 : Initial input 1 : Output 2 : Entrainment *a* : Annulus *ai* : Air reactor *abs* : Absolute
b : Bed or a small space volume *B* : Bubble phase *c* : Core *e* : Emulsion phase
f : Fuel reactor *fuel* : Reactant gas in fuel reactor *g* : Gas *i* : The ith cell *in* : Input
mf :Minimum fluidization O_2 : Oxygen *out* : Output *r* : Recycle *s* : Solid

REFERENCE

[1] Lyngfelt, A., Leckner, B., & Mattisson, T. (2001). "A fluidized-bed combustion process with inherent CO_2 separaton: application of chemical-looping combustion." Chemical Engineering Science 56: 3103-3113.

[2] Kronberger, B., Johansson E., Loffler G., Mattisson T., Lyngfelt A. & Hofbauer H. (2004). "A two-compartment fluidized bed reactor for CO_2 capture by chemical-looping combustion." Chem. Eng. Technol. 27(12): 1318-1326.

[3] Kronberger, B., Lyngfelt, A., Loffler, G. & Hofbauer, H. (2005). "Design and fluid dynamic analysis of a bench-scale combustion system with CO_2 separaation-chemical-looping combustion." Ind. Eng. Chem. Res. 44(3): 546-556.

[4] Adanez, Juan; Garcia-Labiano, Francisco; de Diego, Luis F.; Plata, Ainhoa; Celaya, Javier; Gayan, Pilar; Abad, Alberto (2003), Proceedings of the International Conference on Fluidized Bed Combustion, 17th: 173-182.

[5] Ramkrishna, D. & Mahoney, A. W. (2002). "Population balance modeling. Promise for the future." Chemical Engineering Science 57:595–606.

[6] Ishida, M., Jin, H. & Okamoto, T., (1996). "A fundamental study of a new kind of medium material for chemical-looping combustion." Energy & Fuels 10: 958-963.

[7] Levenspiel, O., Kunii, D. & Fitzgerald, T. (1968) "The processing of solids of changing size in bubbling fluidized beds." Powder Technology 2: 87-96.

[8] Loffler, G., Kaiser, S., Bosch, K. & Hofbauer, H. (2003) "Hydrodynamics of a dual fluidized-bed gasifier – part I: simulation of a riser with gas injection and diffuser." Chemical Engineering Science 58: 4197-4213.

[9] Donald R. van der Varrt (1992) "Mathematical modeling of methane combustion in a fluidized bed." Ind. Eng. Chem. Res. 31: 999-1007.